Contrib Mineral Petrol (2006) 152:639–647
DOI 10.1007/s00410-006-0133-0

ORIGINAL PAPER

Zr diffusion in titanite

D. J. Cherniak

Received: 9 February 2006 / Accepted: 9 August 2006 / Published online: 7 September 2006

Abstract Chemical diffusion of Zr under anhydrous, pO_2-buffered conditions has been measured in natural titanite. The source of diffusant was either zircon powder or a ZrO_2–Al_2O_3–titanite mixture. Experiments were run in sealed silica glass capsules with solid buffers (to buffer at NNO or QFM). Rutherford Backscattering Spectrometry (RBS) was used to measure diffusion profiles. The following Arrhenius parameters were obtained for Zr diffusion parallel to *c* over the temperature range 753–1,100°C under NNO-buffered conditions: $D_{Zr} = 5.33 \times 10^{-7}$ exp(–325 ± 30 kJ mol^{-1}/RT) m^2 s^{-1} Diffusivities are similar for experiments buffered at QFM. These data suggest that titanite should be moderately retentive of Zr chemical signatures, with diffusivities slower than those for O and Pb in titanite, but faster than those for Sr and the REE. When applied in evaluation of the relative robustness of the recently developed Zr-in-titanite geothermometer (Hayden and Watson, Abstract, 16th V.M. Goldschmidt Conference 2006), these findings suggest that Zr concentrations in titanite will be less likely to be affected by later thermal disturbance than the geothermometer based on Zr concentrations in rutile (Zack et al. in Contrib Mineral Petrol 148:471–488, 2004; Watson et al. in Contrib Mineral. Petrol, 2006), but much less resistant to diffusional alteration subsequent to crystallization than the Ti-in-Zircon geothermometer (Watson and Harrison in Science 308:841–844, 2005).

Communicated by T.L. Grove.

D. J. Cherniak (✉)
Department of Earth and Environmental Sciences,
Rensselaer Polytechnic Institute,
Troy, NY 12180, USA
e-mail: chernd@rpi.edu

Introduction

Titanite (sphene) is an accessory mineral widely found in igneous and metamorphic rocks. Because it can include U, Th, REE as well as high field strength elements as substituents in its lattice, it plays an important role as carrier of trace elements useful as petrogenetic indicators and in geochronology.

Zr can be present in fairly high concentrations in titanite. For example, titanites in lamprophyres (Seifert and Kramer 2003) have been found to be among those with the highest Zr concentrations, containing on order of 6 wt% ZrO_2. Chakhmouradian and Zaitasev (2002) have found high Zr concentrations (up to 7.6 wt%) in titanites from the ultramafic–alkaline–carbonatitic Afrikanda complex. Zr-rich titanites are also found in foid-bearing alkaline rocks (e.g., Smith 1970; Giannetti and Luhr 1983; Flohr and Ross 1990; Woolley et al. 1992; Dawson et al. 1994; Della Ventura et al. 1999).

Zr substitutes on the Ti site in titanite. Both a simple direct substitution, i.e., $Ti^{+4} \Leftrightarrow Zr^{+4}$ (Sahama 1946; Della Ventura et al. 1999) and a coupled substitution involving Al and Fe (to minimize lattice distortion), i.e., $Ti^{+4} + Al^{+3} \Leftrightarrow Zr^{+4} + Fe^{+3}$ (Seifert and Kramer 2003) have been proposed as dominant mechanisms. Zoning of Zr on the scale of a few microns has been observed in lamprophyritic titanite (Seifert and Kramer 2003); minor zoning has been attributed to small-scale fluctuation in rates of crystal growth and

diffusion, with marked core to rim zoning likely caused by rapid decrease of temperatures of uprising magma leading to variations in Zr mobility in melts. The degree and scale of zoning may therefore provide insight into magmatic histories and other changes in the geochemical and thermal environment, and Zr diffusivites can assist in further refining this understanding.

In this work, we measure the diffusivity of Zr in natural titanite. Given the development of a geothermometer employing Zr concentrations in titanite (Hayden and Watson 2006) these data have considerable potential for application in evaluating the relative robustness of this geothermometer and the resistance of Zr signatures to later thermal readjustment. The data also complement earlier diffusion measurements of other trace and minor elements in titanite, and permit further insights into substitutional processes in this mineral.

Experimental procedure

The mineral specimens used in this study were from a natural titanite from Minas Gerais, Brazil. Specimens from this locality have been used previously in our studies of Pb (Cherniak 1993) and Sr and Nd (Cherniak 1995) diffusion, and in studies of oxygen diffusion as well (Zhang et al. 2006).

The titanite was cut normal to *c* and polished to 0.3 μm alumina, followed by a chemical polish with colloidal silica. Following polishing, samples were cleaned ultrasonically in distilled water and ethanol and then pre-annealed for 2 days at 900°C in sealed silica capsules with a nickel–nickel oxide (NNO) or quartz–fayalite–magnetite (QFM) buffer, using the same buffer to be used in the diffusion anneals. The purpose of the anneals was both to repair possible surface damage produced by cold-working of the polished samples, and to equilibrate point defects to conditions that would be experienced in the experiments.

The source of diffusant for the experiments was a fine powder of synthetic zircon, obtained from a commercial supplier (Alfa/Aesar). The zircon powder was dried and pre-fired in air for 1 day at 1,200°C prior to the conduct of experiments. To assemble experiments, the source material was loaded into Ag–Pd capsules with the prepared titanite. The capsules were crimped shut and placed in a silica glass capsules along with solid buffer mixture of either nickel metal powder and nickel oxide powder (NNO) or QFM powders. Inside the silica glass capsules, silica glass chips were placed between the solid buffer and the AgPd capsule containing the source and sample to physically separate the sample and buffer. The assemblies in the silica glass tubes were sealed under vacuum, and annealed in vertical tube furnaces for temperatures ranging from 750 to 1,100°C, and times from fifteen minutes to three months. All of the experiments below 1,100°C were run in Kanthal-wound vertical tube furnaces, with temperatures monitored with type K (chromel–alumel) thermocouples during the course of the anneals; temperature uncertainties are ~ ±2°C. Experiments at 1,100°C were run in Deltech furnaces with $MoSi_2$ heating elements; type S (Pt–Pt10%Rh) thermocouples were used to monitor these experiments, with comparable temperature uncertainty. On completion of the anneals, samples were quenched merely by removing them from furnaces and permitting them to cool in air. Samples were then removed from capsules, freed of residual source material and cleaned ultrasonically in successive baths of distilled water and ethanol.

In order to explore the potential effects of differing substitutional processes on diffusion, an experiment was run using a source containing both Zr and Al, since a coupled substitution involving Al has been proposed as a dominant mechanism for Zr exchange (i.e., $Ti^{+4} + Al^{+3} \Leftrightarrow Zr^{+4} + Fe^{+3}$; Seifert and Kramer 2003). The source was made by combining ZrO_2 and Al_2O_3 powders in a 2:1 molar ratio, grinding under ethanol, and annealing at 1,200°C overnight. This ZrO_2:Al_2O_3 mixture was then combined with ground natural titanite (from the same material as the titanite specimens used in experiments) in a 2:1 (by weight) ratio. The ZrO_2:Al_2O_3:titanite mixture was annealed at 1,200°C for 1 day, cooled, and used in place of the zircon powder in the same experimental assembly as employed in the NNO-buffered experiments described above. Since the natural titanite in the sample and source material contain Fe, all of the components needed for the coupled substitution are present in the system.

RBS analysis

RBS has been used in many diffusion studies, including studies of Sr and Nd (Cherniak 1995) and Pb (Cherniak 1993) diffusion in titanite. The analytical approach used here is similar to that used in these studies, with 2 or 3 MeV $^4He^+$ beams used for analysis. Spectra were converted to Zr concentration profiles employing procedures comparable to those outlined in these publications. The resultant profiles were fit with a model to determine the diffusion coefficient (D).

Diffusion is modeled as simple one-dimensional, concentration independent diffusion in a semi-infinite medium with a source reservoir maintained at constant concentration (i.e., a complementary error function solution). The rationale for the use of this model has been discussed in previous publications (e.g., Cherniak and Watson 1992, 1994; Cherniak 1993). Diffusivities are evaluated by plotting the inverse of the error function [i.e., $\mathrm{erf}^{-1}((C_o - C(x,t))/C_o)$] versus depth ($x$) in the sample. A straight line of slope $(4Dt)^{-1/2}$ results if the data satisfy the conditions of the model. C_o, the surface concentration of diffusant, is determined by iteratively varying its value until the intercept of the line converges on zero. In Fig.1, typical diffusion profiles and their inversions through the error function are shown. The uncertainties in concentration and depth from each data point (mainly derived from counting statistics in the former and detector resolution in the latter) were used to evaluate the uncertainties in the diffusivities determined from the fits to the model.

Results

The results from Zr diffusion experiments on titanite, for anneals with NNO and QFM buffers, are presented in Table 1 and plotted in Fig. 2. For the NNO buffered experiments (with transport parallel to c), the Arrhenius parameters derived from a fit to the data are: activation energy 325 ± 30 kJ mol^{-1} and pre-exponential factor 5.33×10^{-7} m^2 s^{-1} (log D_o = –6.27 ± 1.28). Diffusivities for QFM-buffered experiments are similar, yielding an activation energy of 321 ± 34 kJ mol^{-1} and pre-exponential factor 5.26×10^{-7} m^2 s^{-1} (log D_o = –6.27 ± 1.42). While a wide range of fO_2 conditions was not explored since the most geologically relevant data are those that approximate the oxygen fugacity for crustal conditions, it appears that Zr^{+4} diffusion in titanite is relatively insensitive to oxygen fugacity over the investigated fO_2 range.

We performed both ''zero-time'' experiments and a time-series study at 1,000°C under NNO-buffered conditions in order to verify that the measured concentration profiles represent volume diffusion and are not a consequence of other phenomena such as surface reaction that may otherwise result in enhanced Zr yields in the near-surface region. The ''zero-time'' anneal also serves to highlight any systematic problems in the experimental approach. In Fig. 3, the results of the time series at 1,000°C for Zr diffusion parallel to c in titanite are plotted. Diffusivities are quite similar for times ranging over more than an order of magnitude, suggesting that volume diffusion is the dominant

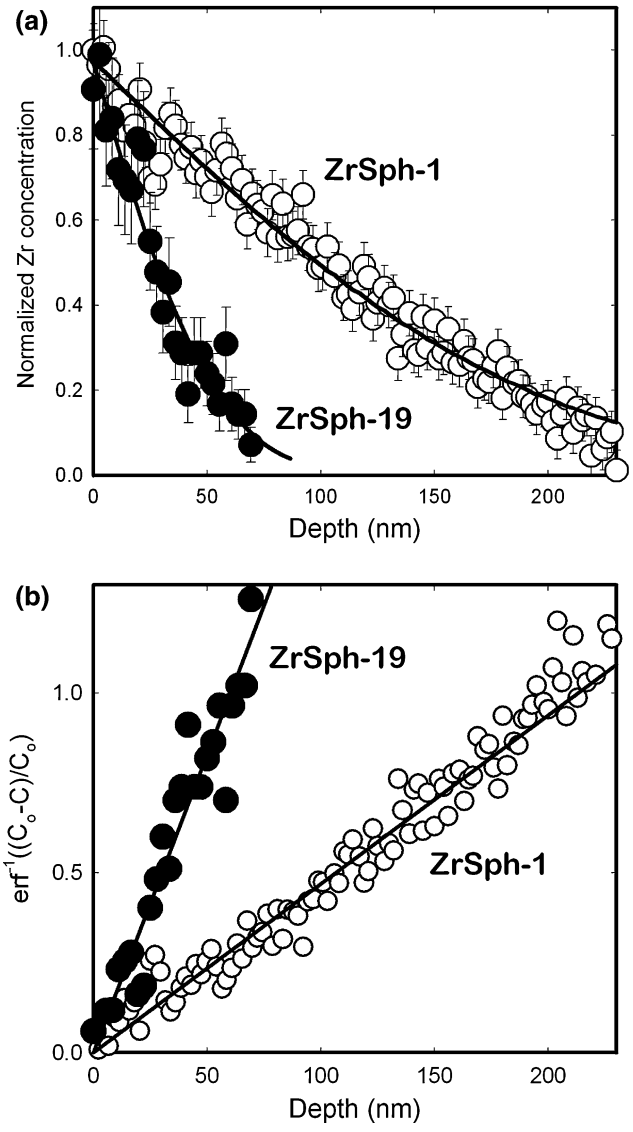

Fig. 1 Typical Zr profiles for titanite. In **a** the measured diffusion profiles are plotted with complementary error function curves. In **b**, the data are linearized by inversion through the error function. Slope of the line is equal to $(4Dt)^{-1/2}$

contributor to the observed diffusion profiles. The zero-time experiment (not plotted), performed by heating a prepared sample capsule up to run temperature and immediately quenching, displays little evidence of significant near-surface Zr during the heatup and quench phases of the anneal, again pointing to the above conclusion.

The experiment run with the ZrO_2–Al_2O_3–titanite source yields a diffusivity similar to that for experiments run with the zircon source, suggesting that diffusion is likely rate-limited by the exchange of Zr^{+4} so that the coupled substitutional mechanism possible when Al is present has little influence on the magnitude of Zr diffusivities.

Table 1 Zr diffusion in titanite

	T (°C)	Time (s)	Source	Buffer	D (m^2 s^{-1})	log D	±
Parallel to *c*							
ZrSph-21	753	7.96×10^6	Zircon	NNO	3.46×10^{-23}	–22.46	0.34
ZrSph-14	802	5.52×10^6	Zircon	NNO	1.22×10^{-22}	–21.91	0.31
ZrSph-4	854	1.38×10^6	Zircon	QFM	7.88×10^{-22}	–21.10	0.42
Zrsph-19	853	2.25×10^6	Zircon	NNO	4.05×10^{-22}	–21.39	0.24
ZrSph-2	900	6.09×10^5	Zircon	QFM	1.35×10^{-21}	–20.87	0.29
ZrSph-10	895	5.18×10^5	Zircon	NNO	1.71×10^{-21}	–20.77	0.14
ZrSph-3	950	1.64×10^5	Zircon	QFM	1.00×10^{-20}	–20.00	0.12
ZrSph-11	950	2.59×10^5	Zircon	NNO	6.13×10^{-21}	–20.21	0.14
ZrSph-1	1,000	2.65×10^5	Zircon	QFM	3.88×10^{-20}	–19.41	0.10
Zrsph-20	1,000	1.82×10^5	Zircon	NNO	1.98×10^{-20}	–19.70	0.25
Zrsph-16	1,000	5.08×10^5	Zircon	NNO	2.50×10^{-20}	–19.60	0.31
Zrsph-17	1,000	6.48×10^4	Zircon	NNO	3.30×10^{-20}	–19.48	0.30
ZrSph-23	1,003	3.17×10^5	Zr–Al[a]	NNO	1.49×10^{-20}	–19.83	0.13
Zrsph-15	1,050	1.53×10^4	Zircon	NNO	1.21×10^{-19}	–18.92	0.31
ZrSph-6	1,096	7.20×10^3	Zircon	QFM	2.44×10^{-19}	–18.61	0.15
ZrSph-12	1,100	9.00×10^3	Zircon	NNO	2.78×10^{-19}	–18.56	0.36

[a] Source material: ZrO_2 + Al_2O_3 + titanite

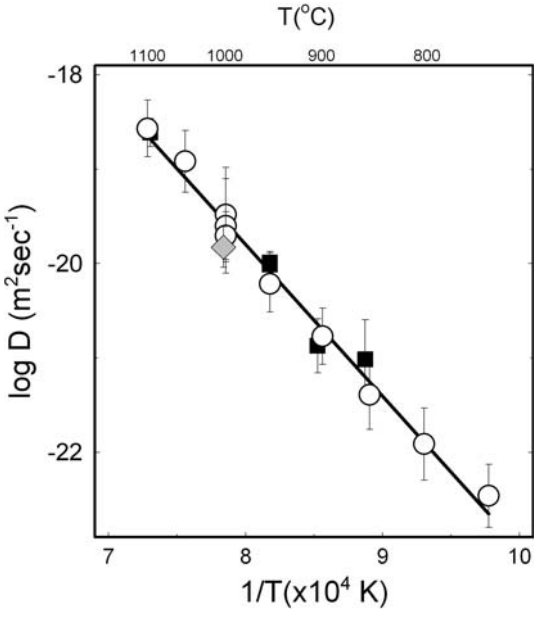

Fig. 2 **a** Arrhenius plot of Zr diffusion data for titanite, showing diffusivities for anneals under both NNO (*circles*) and QFM buffers (*black squares*), and an experiment run using a ZrO_2:Al_2O_3 source (*grey diamond*) with the NNO buffer. Diffusivities for experiments under both QFM and NNO-buffered conditions are similar, suggesting little sensitivity of Zr diffusion to the oxygen fugacity of the system. From a fit with the NNO-buffered data, we obtain the Arrhenius relation $5.33 \times 10^{-7}\exp(-325 \pm 30$ kJ mol^{-1}/RT) m^2 s^{-1}. Diffusivities for QFM-buffered experiments are similar, yielding an activation energy of 321 ± 34 kJ mol^{-1} and pre-exponential factor 5.26×10^{-7} m^2 s^{-1}. Diffusion coefficients for experiments using the ZrO_2:Al_2O_3 and zircon are also of similar value

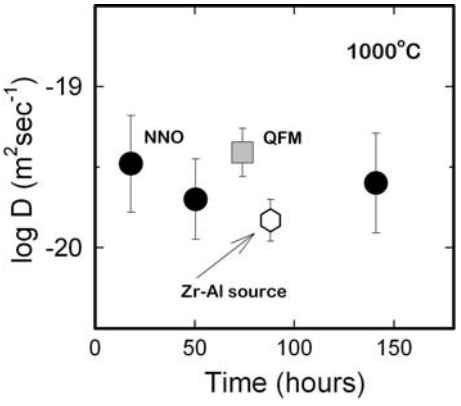

Fig. 3 Time series for Zr diffusion in titanite for anneals at 1,000°C with a NNO buffer. Also shown for comparison is the diffusivity for an experiment run under a QFM buffer, and that for the experiment run using the ZrO_2–Al_2O_3–titanite source. Diffusion rates are quite similar, despite differences in anneal times ranging over about an order of magnitude, suggesting that the dominant process being measured is volume diffusion

Recent experimental work has evaluated the temperature and pressure dependence of Zr partitioning into titanite, with a view toward developing a sensitive and versatile geothermometer (Hayden and Watson 2006). From experimental determinations, the following relation has been developed, relating the logarithm of Zr concentration to T and P:

$$\text{Log Zr concentration} = 12.090 - (9815/T) - (0.0786P),$$

where T is the temperature in Kelvin, P is pressure in kbars, and the Zr concentration is in wt ppm. Measurements of Zr concentrations in natural samples of rhyolites and from the Catalina Schist where T and P are well constrained are in good agreement with this experimentally-determined relation. The values for surface concentrations measured for the diffusion

profiles, when adjusted to the appropriate temperature and pressure, fall along or below this line. That the equilibrium partitioning values form an upper bound for Zr concentrations from the diffusion experiments makes sense in view of the discrete point contacts on the sample surface made by the powder sources (as opposed to a ''continuous'' source) used in the diffusion experiments; however, it should be stressed that the sample-source configuration used in the present work introduces insignificant error in measured diffusivities when compared with the model of a continuous surface source (e.g., Cherniak 2003).

Geological implications

Preservation of Zr signatures in titanite and rutile, and implications for Zr thermometry

Figure 4 presents a summary of extant data for diffusion of Zr (and Hf) in accessory minerals. These data can be considered in light of the development of geothermometers employing these accessory minerals—i.e., Zr in rutile (Watson et al. 2006; Zack et al. 2004; Degeling 2003) Ti in zircon (Watson and Harrison 2005), and Zr in titanite (Hayden and Watson 2006), where the relative diffusivities can provide insight into the robustness of these geothermometers.

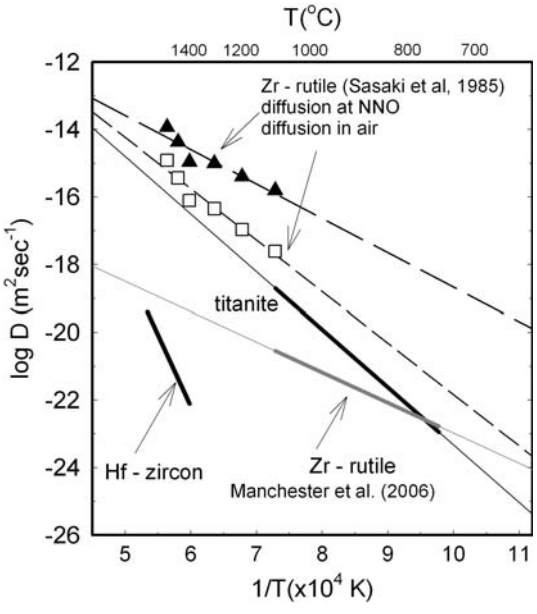

Fig. 4 Zr diffusion in rutile and Hf in zircon, compared with Zr diffusion in titanite. Sources for data: Zr—rutile: Manchester et al. (2006), Sasaki et al. (1985); Hf—zircon: Cherniak et al. (1997)

Diffusion of Hf, like other tetravalent cations in zircon, is extremely slow, about 10 orders of magnitude slower than Zr in titanite. Zr diffusion in zircon should be similar, given its similar size and like charge. Preliminary data on Ti diffusion in zircon suggest that diffusivities are somewhat faster (by about three-quarters to one log unit) than Hf diffusion. Zr diffusion in rutile is also slower than in titanite at high temperatures, based on the data of Manchester et al. (2006). In this work, an activation energy for diffusion of 171 ± 30 kJmol^{-1} and pre-exponential factor of 1.0×10^{-14} m^2 s^{-1} are obtained for diffusion parallel to c, over the temperature range 700–1,100°C for experiments run in air. Given the relatively low activation energy for diffusion in rutile, however, Zr diffusion in titanite will be slower than in rutile below 750°C. Earlier data from Sasaki et al. (1985) suggest even faster diffusivities of Zr in rutile. These findings indicate that under a broad range of geologic conditions Zr diffusion in rutile will be faster than in titanite. Hence, in most cases the Zr-in-titanite geothermometer will be intermediate in its ability to preserve past temperatures—more resistant to resetting than Ti-in-zircon, but less so than Zr-in-rutile.

We can use these data to briefly explore the ways in which Zr in titanite might be affected by volume diffusion, and also consider the relative retentivity of Zr chemical signatures when compared with those of rutile, since Zr thermometry has been developed (e.g., Zack et al. 2004; Watson et al. 2006) for both of these Ti-bearing accessory phases. Differences in U–Pb ages of rutile and titanite have, for example, been used to assess cooling histories following metamorphism (e.g., Cox et al. 1998; Möller et al. 2000) and evaluate timing of later thermal events and recrystallization (e.g., Norcross et al. 2000). In a similar vein, it is instructive to assess the relative robustness of Zr geothermometers by examining the resistance of Zr to diffusional alteration with simple calculations evaluating the extent to which grains will chemically equilibrate with their external environments during a thermal event; calculations likewise can be done to evaluate conditions for closure to Zr diffusion, as outlined in the next section. It may be possible to use the Zr diffusion data to refine thermal histories, and better determine intervals of rutile–titanite coexistence.

We consider a simple model in which the titanite grains are spheres with radii a and initial uniform concentration of C_1, and are exposed to a medium with concentration C_0. The solution to the diffusion equation at the center of the spheres can then be derived (e.g., Crank 1975) given these conditions. When the dimensionless parameter Dt/a^2 (where D is the

diffusion coefficient and t is the time) is less than or equal to 0.03, the concentration at the center of the sphere remains unchanged from its initial value. Above 0.03, the concentration at the center of the sphere is affected by the externally imposed concentration C_0. A similar model can be applied for cylindrical geometry (more suited for rutile), where a is the radius of the cylinder; in this case the dimensionless parameter will be about 0.04.

In Fig. 5 we plot curves representing these dimensionless parameters, with an effective diffusion radius of 250 μm. The calculated curve for titanite is plotted for comparison against a curve for Zr in rutile, using the diffusion parameters from Manchester et al. (2006). These curves define the time–temperature limits under which initial Zr compositional information will be retained in each of these phases. For times and temperatures below the curves, Zr concentrations at crystal cores will remain unaffected, but will be influenced by the concentration of Zr in the surrounding medium when conditions above the curves exist.

Zr will equilibrate under more rapidly in titanite at high temperatures, but more slowly at lower temperatures (below ~780°C) than rutile. For example, at 700°C, 0.5 mm diameter titanite grains will equilibrate with Zr in the surrounding environment in about 50 million years; about 10 Ma would be required for rutile.

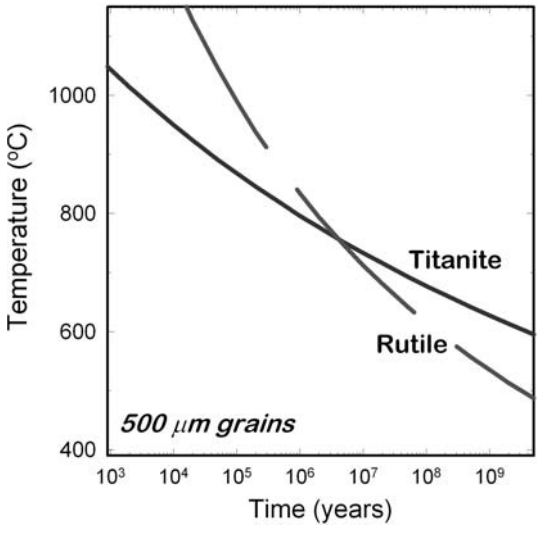

Fig. 5 Conditions for diffusional Zr loss in titanite and rutile for grains of effective diameters of 0.5 mm. Curves represent time–temperature conditions above which the minerals will lose Zr compositional information at the center of grains

Closure temperatures

We can use our experimentally-determined Zr diffusion parameters to calculate closure temperatures for titanite as a function of effective diffusion radius and cooling rate, to evaluate temperatures below which alteration of Zr signatures through volume diffusion will essentially cease to occur. The closure temperature equation (Dodson 1973) is

$$\frac{E}{RT_c} = \ln\left(\frac{ART_c^2 D_0/a^2}{E\mathrm{d}T/\mathrm{d}t}\right), \quad (1)$$

where E and D_o are the activation energy and pre-exponential factors for diffusion of the relevant species, $\mathrm{d}T/\mathrm{d}t$ is the cooling rate, a is the effective diffusion radius, and A is a geometric factor. The derivation of the above expression rests on several assumptions (Dodson 1973, 1986); among these is the condition that at peak temperature T_o, the mineral grain is not retentive of the daughter product over short timescales. This assumption, which makes T_c independent of T_o, is, as Ganguly et al. (1998) note, not satisfied for slowly diffusing species. This condition is not necessarily satisfied for Zr in titanite, nor can it even be assumed that homogeneity is achieved at peak metamorphic temperatures. However, when the dependence of T_c on T_o is taken into account in calculating closure temperatures, the deviations of T_c from conventional closure temperatures calculated using Eq. 1 are smaller with increasing peak temperature (T_o) and slower cooling rate (Ganguly et al. 1998; Ganguly and Tirone 1999). The geometric factor, A, in Dodson's expression of mean closure temperature above, is equal to $\exp(G)$, where G is the value of the closure function, $G(x)$, spatially averaged over the crystal. In deriving the expression for $G(x)$, and ultimately A, the dimensionless parameter M [where M is defined as equal to $D(T_o)RT^2/(Ea^2\mathrm{d}T/\mathrm{d}t)$], is much greater than 1 (Dodson 1986). For smaller values of M, another term, $g(x)$, will become significant, and is summed with G in the exponential expression above to produce the variable A', where $A' = \exp(G(x) + g(x))$, which can be substituted for A in Eq. 1 above. A' will be larger than the value of 55 [i.e., exp (4.0066)] one obtains when the condition of $M >> 1$ is met (i.e., when $g(x) \rightarrow 0$). With increasing A', closure temperature will exhibit greater deviation from Dodson's (1973) classical formulation.

This is illustrated in Fig. 6, where mean closure temperatures for Zr in titanite are plotted as a function of cooling rate for a radius of 500 μm, and spherical geometry (Fig. 6a). Also plotted (Fig. 6b) are mean

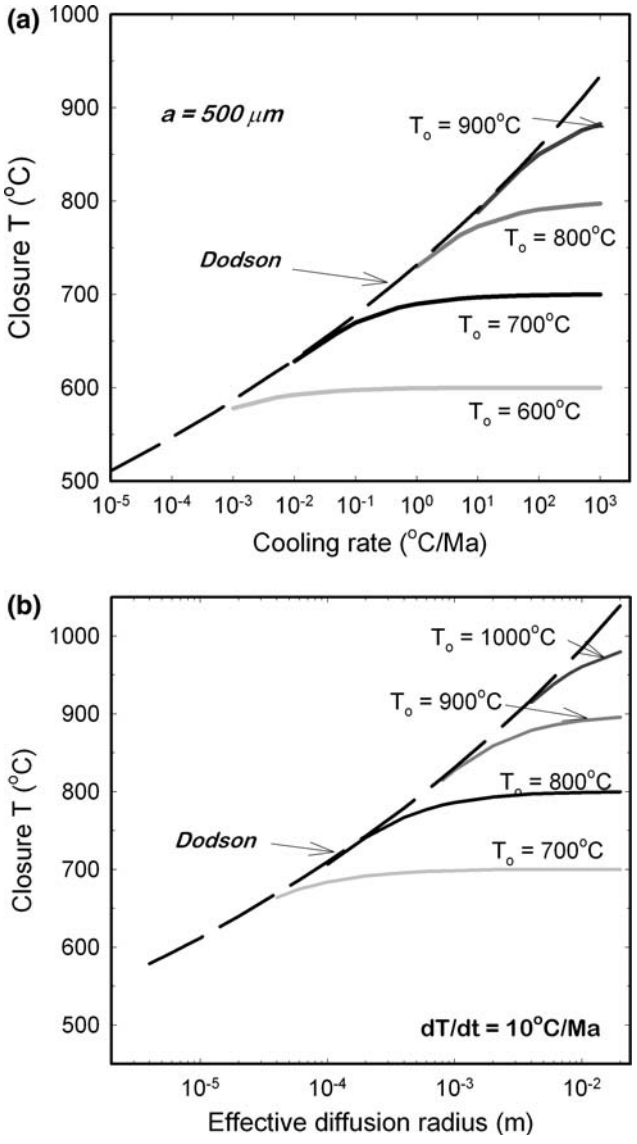

Fig. 6 Mean closure temperatures for Zr in titanite as a function of cooling rate for a fixed grain radius of 500 μm (**a**), and as function of grain radius with a fixed cooling rate of 10°C/Ma (**b**). Closure temperature curves are calculated for a few different peak temperatures (T_o), using the expressions of Ganguly and Tirone (1999), which consider cases of closure with arbitrarily small extent of diffusion. Also plotted are closure temperatures calculated using the classical Dodson (1973) formula (*dashed lines*). Deviations in mean closure temperatures from the Dodson curves can be observed to increase with larger grain radii, faster cooling rates, and decreasing peak temperatures. Spherical geometry was used in all calculations

closure temperatures as a function of grain radius for a cooling rate of 10°C/Ma. In each case, curves for four different values of T_o are shown, which have been calculated using the extension of the Dodson formulation from Ganguly and Tirone (1999), using software developed by these authors. These curves are plotted with those calculated using the conventional Dodson (1973) expression (Eq. 1). For small grain radii, slow cooling rates, and comparatively high peak temperatures, the former closure temperature curves will converge upon the Dodson values, but significant deviations can exist for larger grains, fast cooling rates, and lower peak temperatures. Given typical titanite grain sizes and Zr diffusivities, departure from Dodson values may not be uncommon.

Relative retentivity of Pb, and O isotope, and REE and Zr zoning

Data for diffusion of various cations and oxygen in titanite are plotted in Fig. 7. Diffusion of Zr is about an order of magnitude faster than Sr^{+2}, while about two orders of magnitude slower than Pb^{+2}. Diffusion of Zr is more than two orders of magnitude faster than diffusion of the REE^{+3} in titanite. Diffusion of oxygen, under both dry and hydrothermal conditions, is faster than diffusion of Zr.

However, it should be stressed that the REE and divalent cations substitute for Ca^{+2} in the titanite lattice (e.g. Hughes et al. 1997; Ribbe 1980; Higgins and Ribbe 1976) and Zr substitutes for Ti on a different lattice site, so it would not be expected that diffusivities of these species could be compared in order to assess any potential correlations of diffusivities with

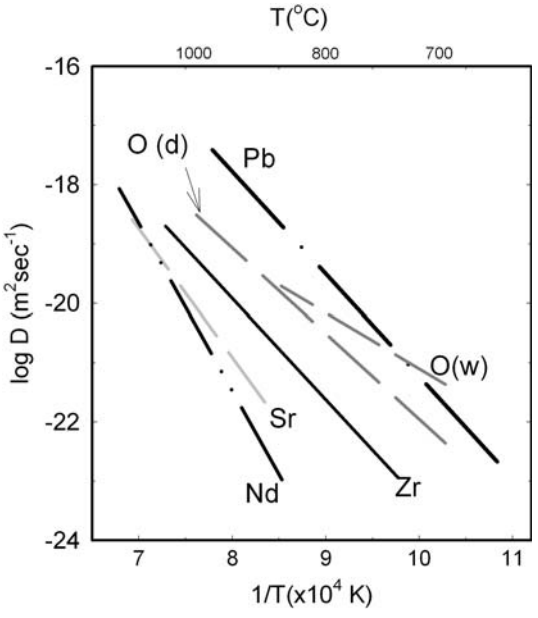

Fig. 7 Arrhenius plot of diffusion data for cation and anion diffusion in titanite. Sources for data: Nd, Sr: Cherniak (1995); Pb: Cherniak (1993); O: Zhang et al. (2006). For oxygen, Arrhenius relations are plotted for both dry (*d*) and hydrothermal (*w*) conditions

cation size and charge. Nonetheless, the relative rates of diffusion of these important geochemical tracers can be considered with respect to the possible retention or diffusional loss of chemical signatures, as will be discussed below.

Zr can be compositionally zoned in titanite, as can other trace and minor elements of geochemical interest. Sector zoning of the REE, Y, Nb, Al and Fe, for example, is observed in titanite (e.g., Paterson and Stephens 1992). Therefore it is useful to consider the conditions under which such zoning may be lost. Ideally, it may be possible to qualitatively evaluate the degree of diffusive exchange by assessing the dimensions of zones and variation in Zr content (analyzed via electron or ion microprobe, for example) across a titanite grain.

We consider a simple model, with zones in a titanite modeled as plane sheets of thickness l; adjacent planes have different concentrations of diffusant. Only diffusion normal to the planar interface is considered. A (somewhat arbitrary) criterion for alteration of zones is employed. Zones are considered to be "lost" if a compositional change of 10% is attained in the zone's center; the dimensionless parameter Dt/l^2 will be equal to 3.3×10^{-2} when this condition occurs.

Figure 8 shows curves constraining the time–temperature conditions under which Zr zoning of 5 and 50 m scale will be retained in titanite given the above criteria. These are compared with zoning of Pb, REE and oxygen isotopes, obtained from the data of Cherniak (1993, 1995) and Zhang et al. (2006), respectively. In the last case, diffusion data from hydrothermal experiments are used as it is considered more relevant for most geologic conditions; the presence of water can have a significant effect on oxygen diffusion but has been shown to have relatively little effect on cation diffusion (e.g., Cherniak and Watson 2001; Farver and Giletti 1998).

Titanite will be more retentive of Zr than of either O or Pb isotopes, but considerably less so than for REE signatures. For example, at 650°C, times for diffusional alteration on the 50 μm scale would be about 10 Ma for Zr, 20,000 years for oxygen, 100,000 years for Pb, but tens of billions of years for the REE. This indicates that information obtained through Zr thermometry and that from U–Pb geochronology may be diffusionally decoupled in titanite, so that there may not always be a correspondence between U–Pb dates and past temperatures extracted from Zr concentrations. This also appears the case for rutile, where Zr diffusion is slower than that of Pb (Manchester et al. 2006; Cherniak 2000).

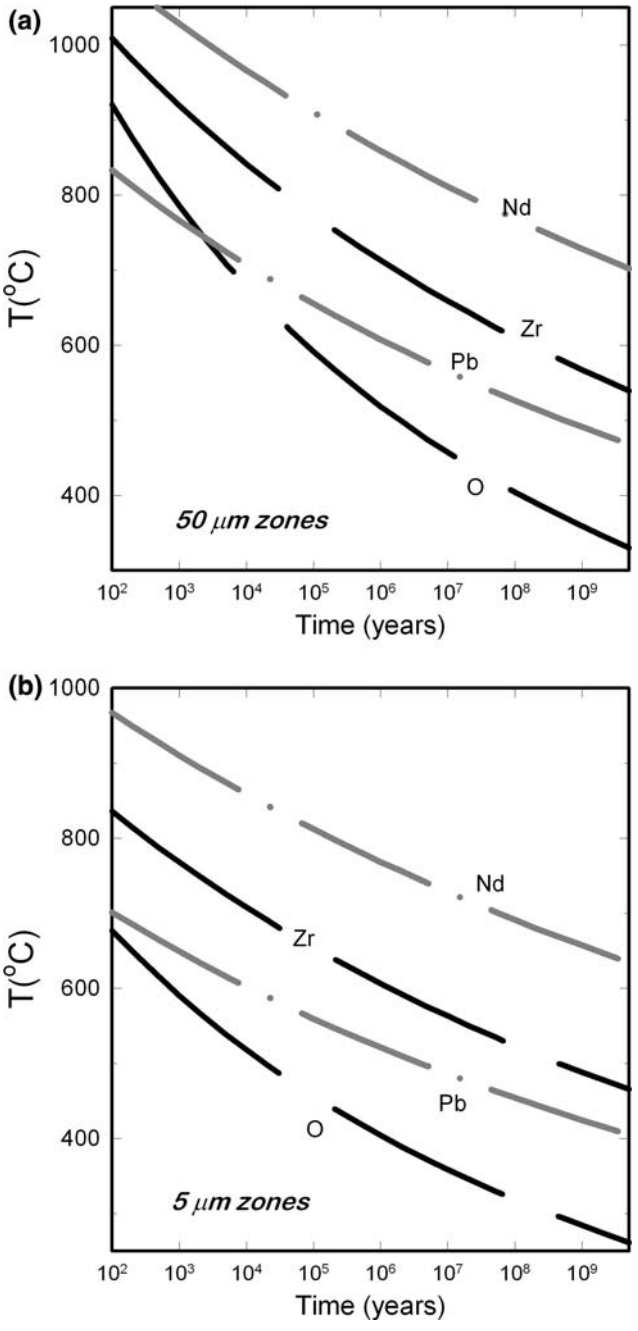

Fig. 8 Preservation of Zr zoning in titanite. The curves plotted represents maximum time–temperature conditions under which 5 and 50 μm zoning in Zr will be preserved in titanite. For conditions above the curve, well-defined zoning on these scales will be lost. Also plotted for comparison are curves for Nd, Pb and oxygen, calculated using the Arrhenius relations plotted in Fig. 7

Acknowledgments Thanks to Bruce Watson for helpful discussion during the course of this work. Thanks to Janet Manchester for sharing information from her diffusion study of Zr and Hf in rutile. The comments of an anonymous reviewer assisted in improvement of the manuscript. This work was supported by grant EAR-0440228 from the National Science Foundation (to E.B. Watson).

References

Chakhmouradian AR, Zaitsev AN (2002) Calcite–amphibole–clinopyroxene rock from the Afrikanda complex, Kola Peninsula, Russia: morphology and a possible link to carbonatites: III. Silicate minerals. Can Mineral 40:1347–1374

Cherniak DJ (1993) Lead diffusion in titanite and preliminary results on the effects of radiation damage on Pb transport. Chem Geol 110:177–194

Cherniak DJ (1995) Sr and Nd diffusion in titanite. Chem Geol 125:219–232

Cherniak DJ (2000) Pb diffusion in rutile. Contrib Mineral Petrol 139:198–207

Cherniak DJ (2003) Silicon self-diffusion in single-crystal natural quartz and feldspar. Earth Planet Sci Lett 214:655–668

Cherniak DJ, Watson EB (1992) A study of strontium diffusion in K-feldspar, Na–K feldspar and anorthite using Rutherford Backscattering Spectroscopy. Earth Planet Sci Lett 113:411–425

Cherniak DJ, Watson EB (1994) A study of strontium diffusion in plagioclase using Rutherford Backscattering Spectroscopy. Geochim Cosmochim Acta 58:5179–5190

Cherniak DJ, Watson EB (2001) Pb diffusion in zircon. Chem Geol 172:5–24

Cherniak DJ, Hanchar JM, Watson EB (1997) Diffusion of tetravalent cations in zircon. Contrib Mineral Petrol 127:383–390

Cox RA, Dunning GR, Indares A (1998) Petrology and U–Pb geochronology of mafic, high-pressure, metamorphic coronites from the Tshenukutish domain, eastern Grenville Province. Precamb Res 90:59–83

Crank J (1975) The mathematics of diffusion, 2nd edn. Oxford University Press, New York, pp 414

Dawson JB, Smith JB, Steele IM (1994) Trace-element distribution between coexisting perovskite, apatite, and titanite from Oldoinyo Lengai. Tanzania Chem Geol 117:285–290

Degeling HS (2003) Zr equilibria in metamorphic rocks. Unpublished PhD thesis, Australian National University, 231 p

Della Ventura G, Bellatreccia F, Williams CT (1999) Zr- and LREE-rich titanite from Tre Croci, Vico Volcanic complex (Latium Italy). Mineral Mag 63:123–130

Dodson MH (1973) Closure temperature in cooling geochronological and petrological systems. Contrib Mineral Petrol 40:259–274

Dodson MH (1986) Closure profiles in cooling systems. Mat Sci Forum 7:145–154

Farver JR, Giletti BJ (1998) Strontium diffusion kinetics in apatite. Eos Trans Am Geophys Union 79(17Suppl):369

Flohr JK, Ross M (1990) Alkaline igneous rocks of Magnet Cove, Arkansas: mineralogy and geochemistry of syenites. Lithos 26:67–98

Ganguly J, Tirone M (1999) Diffusion closure temperature and age of a mineral with arbitrary extent of diffusion: theoretical formulation and applications. Earth Planet Sci Lett 170:131–140

Ganguly J, Tirone M, Hervig RL (1998) Diffusion kinetics of samarium and neodymium in garnet, and a method for determining cooling rates of rocks. Science 281:805–807

Giannetti B, Luhr LF (1983) The white trachytic tuff of Roccamonfina Volcano (Roman Region, Italy). Contrib Mineral Petrol 84:235–252

Hayden L, Watson EB, Wark DA (2006) A thermobarometer for sphene. Abstract, 16th V.M. Goldschmidt Conference

Higgins JB, Ribbe PH (1976) The crystal chemistry and space groups of natural and synthetic titanites. Am Miner 61:878–888

Hughes JM, Bloodaxe ES, Hanchar JM, Foord EE (1997) Incorporation of rare earth elements in titanite: stabilization of the A2/a dimorph by creation of antiphase boundaries. Am Miner 82:512–516

Manchester J, Cherniak DJ, Watson EB (2006) Zr and Hf diffusion in rutile (in preparation)

Möller A, Mezger K, Schenk V (2000) U-Pb dating of metamorphic minerals: Pan-African metamorphism and prolonged slow cooling of high pressure granulites in Tanzania East Africa. Precamb Res 104:123–146

Norcross C, Davis DW, Spooner ETC, Rust A (2000) U–Pb and U–Pb age constraints on Paleoproterozoic magmatism, deformation and gold mineralization in the Omai area. Guyana Shield Precamb Res 102:69–86

Paterson BA, Stephens WE (1992) Kinetically induced compositional zoning in titanite: implications for accessory-phase/melt partitioning of trace elements. Contrib Mineral Petrol 109:373–385

Ribbe PH (1980) Titanite In: Ribbe PH (ed) Orthosilicates, reviews in mineralogy, vol 5. Mineralogical Society of America, Washington, pp 137–154

Sahama ThG (1946) On the chemistry of the mineral titanite. Bull Comm Goelo Finl 138:88–120

Sasaki J, Peterson NL, Hoshino K (1985) Tracer impurity diffusion in single-crystal rutile (TiO_{2-x}). J Phys Chem Solids 46:1267–1283

Seifert W, Kramer W (2003) Accessory titanite: an important carrier of zirconium in lamprophyres. Lithos 71:81–98

Smith AL (1970) Sphene, perovskite, and coexisting Fe–Ti oxide minerals. Am Mineral 55:264–269

Watson EB, Harrison TM (2005) Zircon thermometer reveals minimum melting conditions on earliest Earth. Science 308:841–844

Watson EB, Wark DA, Thomas JB (2006) Crystallization thermometers for zircon and rutile. Contrib Mineral Petrol (in press)

Woolley AR, Platt RG, Eby N (1992) Niobian titanite and eudialyte from the Ilomba nepheline syenite complex, north Malawi. Mineral Mag 56:428–430

Zack T, Moraes R, Kronz A (2004) Temperature dependence of Zr in rutile: empirical calibration of a rutile thermometer. Contrib Mineral Petrol 148:471–488

Zhang XY, Cherniak DJ, Watson EB (2006) Oxygen diffusion in titanite: lattice diffusion and fast-path diffusion in single crystals. Chem Geol (in press)